Raman and IR Spectroscopy of Silver Iodide/Silver Selenate Fast Ion-Conducting Glasses†

Cornelia Cramer

Institut für Physikalische Chemie, Universität Münster, D-48149 Münster, Germany

Marcos Grimsditch and Marie-Louise Saboungi*

Argonne National Laboratory, Argonne, Illinois 60439

Received: August 24, 1998; In Final Form: November 16, 1998

We report IR and Raman spectra obtained on a highly ion-conducting glass-forming system, $x(AgI)_2 \cdot (1 - x)Ag_2SeO_4$ with $x = 0.35, 0.40, 0.46, 0.48, 0.50, 0.54$. For $0.48(AgI)_2 \cdot 0.52Ag_2SeO_4$, spectra were recorded in a temperature range between room temperature and 573 K, probing the glassy, partly crystallized, and molten states of the material. The spectra of the glasses are compared with those of the crystalline compounds Ag_2SeO_4 and α-AgI. Conclusions reached from the present work are consistent with those recently derived from neutron diffraction and dynamic conductivity measurements on the same materials.

Introduction

In the class of solid fast ion conductors, the high-temperature phase of silver iodide, α-AgI, plays an outstanding role because of its extraordinarily high ionic d.c. conductivity, which exceeds $1\ \Omega^{-1}\ cm^{-1}$. In amorphous ion conductors, it is possible to reach relatively high conductivities, about $10^{-2}\ \Omega^{-1}\ cm^{-1}$ at room temperature, by introducing silver iodide into the glass matrix. Whereas ion conduction is well understood in crystalline compounds, many questions related to ion dynamics in glasses remain a challenge due to the lack of long-range order. In principle, combined studies of temperature and compositional dependence of structure and dynamics should elucidate the outstanding questions.[1] Here, we report on Raman and IR spectra of $x(AgI)_2 \cdot (1 - x)Ag_2SeO_4$ which forms ionic glasses containing discrete Ag^+, I^-, and SeO_4^{2-} ions. As noted previously,[2,3] we use the nomenclature $(AgI)_2$ so that both components contain equal amounts of silver ions. Neither AgI nor Ag_2SeO_4 forms glasses, but mixtures in a limited concentration range can be readily quenched[4−7] to a glassy state with remarkably low glass transition temperatures, T_g, ranging from 350 to 295 K.[5,7] At temperatures about 30 K above T_g, the glasses tend to crystallize and the conductivity drops by about an order of magnitude.[8]

On the basis of static structure factors previously measured for $x(AgI)_2 \cdot (1 - x)Ag_2SeO_4$ glasses, a structural model has been developed which is schematically presented in Figure 1. According to this model, the glass structure can be formally constructed from the face-centered orthorhombic lattice of crystalline silver selenate by replacing a fraction x of SeO_4^{2-} ions by $2x$ I^- ions. One half of the iodide ions replace the vacated SeO_4^{2-} ions while the other half occupy the vacant tetrahedral sites of the face-centered orthorhombic lattice. (The ionic radius of I^- (2.2 Å) is very similar to that of SeO_4^{2-} (2.4 Å)). On replacing the selenate by iodide ions, two different kinds of regions are formed: regions (I) with low iodide content and strong orientational correlations between neighboring selenate ions; and regions (II) with high iodide content, weaker orientational correlations, and larger average distances between selenate ions.

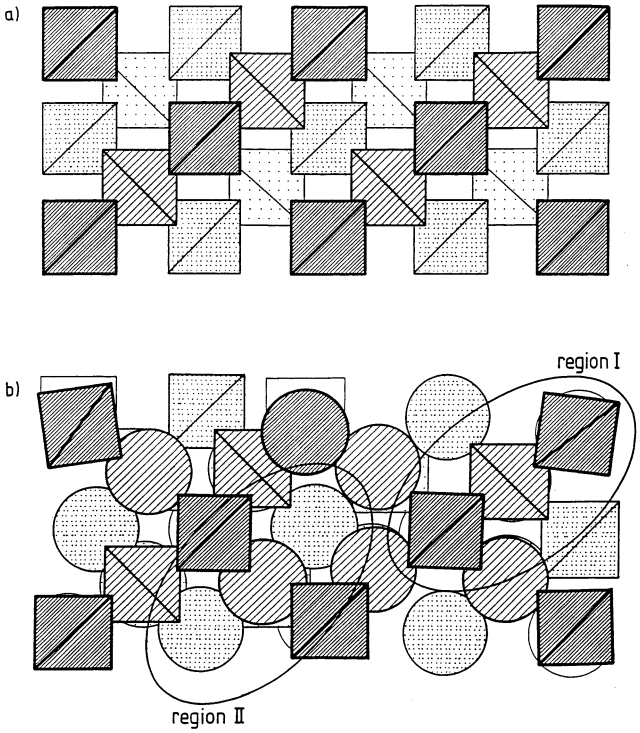

Figure 1. Schematic drawing of the structure of (a) c-Ag_2SeO_4 and (b) $x(AgI)_2 \cdot (1 - x)Ag_2SeO_4$ glass. (a) Shows the selenate tetrahedra of c-Ag_2SeO_4 in a projection into the x,y plane. Tetrahedra at different z-coordinates are represented by different patterns: dense hatching $z = 0$, light hatching $z = c/4$, dense dotting $z = c/2$, and light dotting $z = 3c/4$. In (b) iodide ions are represented by circles. Blank symbols correspond to $z = c$ in the crystal. Regions I and II are defined in the Introduction.

Dynamic conductivity spectra over a range from a few Hz to the THz regime have been reported for $0.48(AgI)_2 \cdot 0.52Ag_2SeO_4$[2] and interpreted in terms of favorable and unfavorable sites for the mobile silver ions. The favorable Ag^+ sites preferably contribute to the long-range ionic transport taking place along

* Corresponding author.

† Dedicated to Charles Austen Angell on the occasion of his 65th birthday.

10.1021/jp983467t CCC: $18.00
Published on Web 01/22/1999

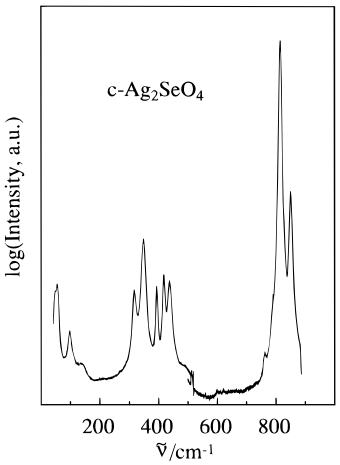

Figure 2. Raman spectrum of c-Ag_2SeO_4 at 298 K.

regions (II). The unfavorable sites, from which the mobile Ag^+ ions jump back into their starting position, produce localized ionic motions in regions (I).

In this paper, we present room temperature Raman spectra of crystalline silver selenate, c-Ag_2SeO_4, and $x(AgI)_2 \cdot (1-x)Ag_2SeO_4$ for $x = 0.35$, 0.40, 0.46, 0.48, 0.50, and 0.54. For $0.48(AgI)_2 \cdot 0.52Ag_2SeO_4$, additional spectra were taken at various temperatures between 298 and 573 K. We compare the Raman spectra with conductivity data obtained by far-infrared spectroscopy and show that the results are consistent with the structural model described above.

Experimental Section

Raman spectra were excited with 568.1 nm radiation from a krypton ion laser. The geometry was near back-scattering and no polarization analyzer was used. The scattered light was analyzed with a triple Jobin-Yvon grating spectrometer and detected with a CCD camera from Princeton Instruments. Since the spectral range of the CCD detection system was limited to 475 cm^{-1} at 568.1 nm, spectra over a wider range were generated as composites of single spectra taken at different spectrometer settings.

For the determination of the conductivity in the IR regime we used a Fourier transform infrared spectrometer (Bomem DA 8.1). To cover a wide frequency range, this spectrometer is equipped with various sources, beam splitters, and detectors. Transmission spectra were taken up to a frequency of roughly 700 GHz using samples of different thickness; the conductivity can be determined by an indirect simulation method described elsewhere.[9,10] Above 700 GHz the conductivity was calculated from reflectance data applying the Kramers−Kronig inversion technique.[11]

The preparation of the glasses is described elsewhere.[2,3] For the Raman measurements, flat glass disks of several millimeters thickness were used at room temperature while rectangular-shaped quartz containers were used for the high-temperature measurements. Thin samples (below 130 μm) made by roller quenching, and cylindrical samples of 12 mm diameter and approximately 8 mm thickness were used for the IR transmission and reflection measurements, respectively.

Results and Discussion

Figure 2 shows the ambient temperature Raman spectrum of c-Ag_2SeO_4 (space group *Fddd*). The peaks at low wavenumbers (49, 56, 98, 139 cm^{-1}) are due to lattice modes as in previous work.[12−14] Further studies (preferably on a single crystal and at lower wavenumbers and with differently polarized light) are needed to unequivocally assign these peaks to special kinds of lattice modes. Peaks above 300 cm^{-1} can be attributed to internal vibrations of the SeO_4^{2-} tetrahedra. Selenate ions in solution (point group T_d) show four kinds of internal vibrations which split into nine Raman active modes in the orthorhombic crystal *Fddd* environment. By comparison with isomorphic compounds like Na_2SO_4(V)[12,13] and Na_2SeO_4,[14] the peaks in c-Ag_2SeO_4 can be assigned to the vibrations presented in Table 1. The most intense peak at 816 cm^{-1} is due to the totally symmetric vibration of the selenate tetrahedron. The wavenumbers of the various bands of silver selenate are found to be smaller by a factor 0.93−0.96 than the corresponding ones of sodium selenate. This could be qualitatively explained by changes in the reduced masses and bonding strengths.

TABLE 1: Internal Vibrations of c-Ag_2SeO_4 and Isomorphic Na_2SeO_4[14]

	$\tilde{\nu}$/cm^{-1}		
mode	SeO_4^{2-} [15]	Na_2SeO_4[14]	Ag_2SeO_4
A_g ($\tilde{\nu}_1$)	835	848	816
A_g ($\tilde{\nu}_2$)	345	337	318
A_g ($\tilde{\nu}_2$)	345	362	349
B_g ($\tilde{\nu}_3$)	875	895	810(s)
B_{2g} ($\tilde{\nu}_3$)	875	901	851
B_{3g} ($\tilde{\nu}_3$)	875	875	830(s)
B_{1g} ($\tilde{\nu}_4$)	416	457	438
B_{2g} ($\tilde{\nu}_4$)	416	453	419
B_{1g} ($\tilde{\nu}_4$)	416	425	395

[a] The wavenumbers of the vibrations of the isolated selenate tetrahedra are specified in the first column. (s) stands for "shoulder".

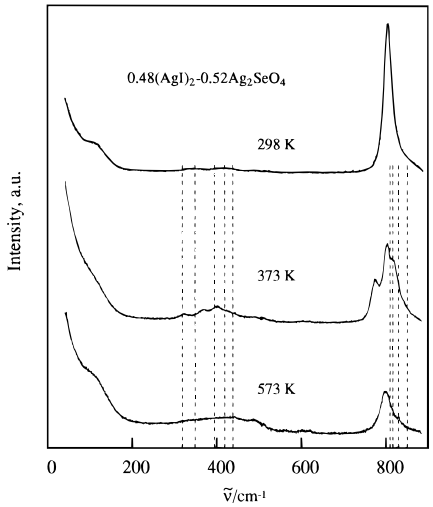

Figure 3. Raman spectra of $0.48(AgI)_2 \cdot 0.52Ag_2SeO_4$ taken at 298, 373, and 573 K. The spectra correspond to the glassy, the partially crystallized, and the molten states. The dashed lines indicate the peak positions found in c-Ag_2SeO_4.

Figure 3 shows Raman spectra of $0.48(AgI)_2 \cdot 0.52Ag_2SeO_4$ corresponding to the glassy state at 298 K, the partially crystallized state at 373 K and the molten state at 573 K. The dashed lines indicate the peak positions found in c-Ag_2SeO_4. Neutron diffraction results on $x(AgI)_2 \cdot (1-x)Ag_2SeO_4$ glasses showed that the selenate ions are regularly shaped tetrahedra with Se−O bond lengths of 1.66 Å. The corresponding length in c-Ag_2SeO_4 is 1.65 Å.[3] The internal vibrations of the SeO_4^{2-} ions present in $x(AgI)_2 \cdot (1-x)Ag_2SeO_4$ glasses give rise to broad peaks at positions close to those of c-Ag_2SeO_4.

In glassy $0.48(AgI)_2 \cdot 0.52Ag_2SeO_4$ the most intense peak (805 cm^{-1}) is caused by the symmetric breathing mode of the selenate tetrahedra. As glasses lack long-range order, no well-defined

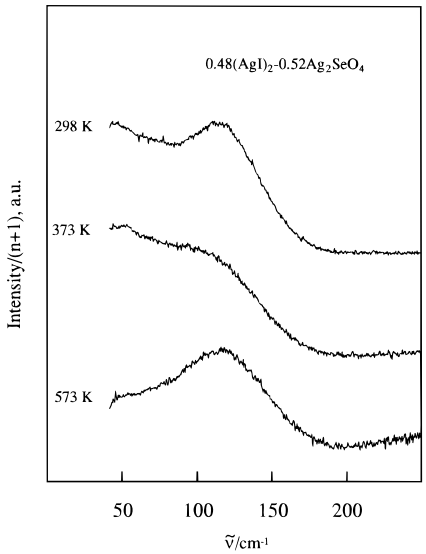

Figure 4. Low-wavenumber range of the normalized Raman spectra of $0.48(AgI)_2{\cdot}0.52Ag_2SeO_4$ at 298, 373, and 573 K.

environment is seen by the SeO_4^{2-} ions, making it impossible to predict the influence of neighboring ions on their internal vibrations. In the partly crystallized state at 373 K the number and positions of peaks are different from those in both the glassy state and the melt, reflecting a change of symmetry in the local environment of the selenate tetrahedra. In addition, the crystalline regions do not consist of pure silver selenate. The overall shape of the Raman spectra of the glass and the melt are very similar except for the breadths and heights of the peaks. This is in good agreement with the static structure factors[3] which clearly showed that the local and even the intermediate-range order in the glasses survive the melting process.

It is interesting to calculate normalized spectra, e.g., the intensity of the observed Stokes lines normalized by the factor $(n(\tilde{\nu}) + 1)$ which is proportional to the matrix element for phonon creation.[16−19] The Bose−Einstein factor $n\ (\tilde{\nu}) = [\exp(ch\tilde{\nu}/(k_BT)) - 1]^{-1}$ reflects the population number of the initial phonon states at a given temperature T, c denotes the speed of light in free space, h is the Planck constant, and k_B is the Boltzmann constant. The normalized low-frequency spectra are shown in Figure 4.The similarity between the Raman spectra of the glass and the melt (taken 260 K above T_g) is also observed in the low-frequency region; the peaks in this region can be attributed to either phonon-like collective modes or localized cation motions in various ionic environments.[20−22] The broad peak at 115 cm^{-1} clearly seen in the glassy and molten states becomes a shoulder in the partly crystallized material. Below 80 cm^{-1} the spectra of both solid samples show an increase in intensity toward lower wavenumbers, whereas the intensity in the spectrum of the melt seems to drop.

We now discuss the peaks at low wavenumbers. The spectra of glassy $x(AgI)_2{\cdot}(1 - x)Ag_2SeO_4$ with $x = 0.35$, 0.40, 0.46, 0.48, 0.50, and 0.54 are compared after dividing by $(n(\tilde{\nu}) + 1)$ and normalizing so that equal intensities are obtained in a wavenumber range between 300 and 450 cm^{-1}, which is equivalent to normalizing to equal amounts of selenate tetrahedra. The resulting spectra in Figure 5 are compared with those of the two crystalline compounds Ag_2SeO_4 at 298 K and α-AgI at 573 K.[23] The shape of the Raman spectra of all glasses shows a striking similarity with the spectrum of α-AgI but differs significantly from that of c-Ag_2SeO_4. The peak at around 118 cm^{-1} for $x = 0.35$ (labeled as $\tilde{\nu}^*$) shifts linearly to lower wavenumbers with increasing AgI content. The peak positions

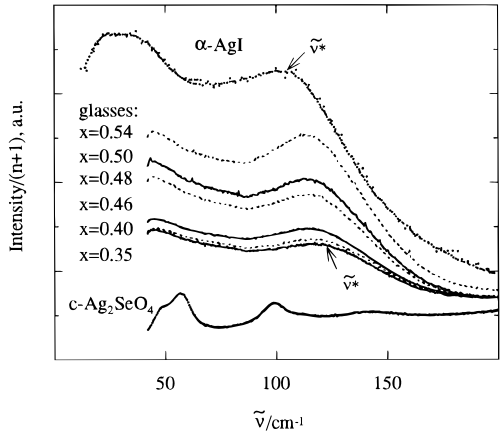

Figure 5. Low-wavenumber range of normalized Raman spectra of $x(AgI)_2{\cdot}(1 - x)Ag_2SeO_4$ at 298 K. For comparison the spectra of c-Ag_2SeO_4 (298 K) and α-AgI (573 K)[23] are also included.

TABLE 2: Peak Positions, $\tilde{\nu}^*$, in the Raman Spectra of Glassy $x(AgI)_2{\cdot}(1 - x)Ag_2SeO_4$ (See Figure 5)

x	$\tilde{\nu}^*/cm^{-1}$	compound
0.35	118 ± 2	glass
0.40	117 ± 2	glass
0.46	116 ± 2	glass
0.48	115 ± 2	glass
0.50	114 ± 2	glass
0.54	113 ± 2	glass
1.00	101 ± 2	extrapolated value, glass
1.00	100	α-AgI[23−25]

for all glass compositions are summarized in Table 2. Extrapolation of $\tilde{\nu}^*$ toward $x = 1.0$ yields a value of 101 ± 2 cm^{-1} for the glassy system. Within experimental error, this value is identical to that of crystalline α-AgI, 100 cm^{-1}.[23−25] This is a strong indication that the low-wavenumber regime in the Raman spectra of the glasses is dominated by vibrations similar to those existing in α-AgI. The approximately linear increase in the peak intensity with AgI content which can only be related to the increasing AgI content supports this conclusion. The similarity between the low-wavenumber regions of Raman spectra of glasses containing AgI and that of α-AgI has been reported earlier.[26,27] However, this is the first time that a quantitative relation between the peak positions and AgI content has been established.

Crystalline α-AgI is a strongly disordered material with a body-centered iodide sublattice and with the silver ions nuclei located in elongated ellipsoidal regions where the tetrahedral site is the equilibrium position.[44] Therefore, in AgI-containing glasses like the borate and phosphate glasses discussed in refs 26 and 27, the silver ions were assumed to be in a tetrahedral environment of the iodide ions, forming α-AgI like clusters. These clusters were believed to be dissolved in the matrix formed by the borate and phosphate network. The existence of such clusters has, however, been discredited by reverse Monte Carlo simulations, see e.g. ref 45, as well as by alternative descriptions of the structure factor of glasses containing AgI.[3]

We now compare the Raman spectra of $0.48(AgI)_2{\cdot}0.52Ag_2SeO_4$ with dynamic conductivity spectra determined by (far)infrared spectroscopy. Figure 6 represents the low-frequency part of the Raman and IR spectra of $0.48(AgI)_2{\cdot}0.52Ag_2SeO_4$ versus the experimental frequency. These spectra are compared with the Raman and IR spectra of crystalline α-AgI.[23,28,29] Above 8 THz, the IR and Raman spectra of $0.48(AgI)_2{\cdot}0.52Ag_2SeO_4$ are determined by internal vibrations of the selenate tetrahedra, which have been discussed before.

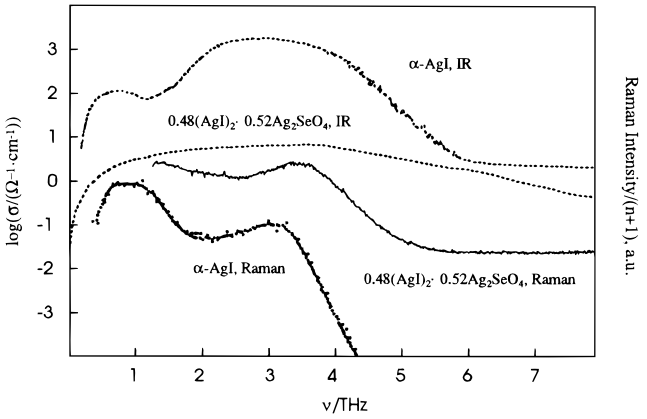

Figure 6. Low-frequency range of IR[2] and normalized Raman spectra of $0.48(AgI)_2 \cdot 0.52Ag_2SeO_4$ at room temperature. For comparison the Raman spectrum of α-AgI (573 K)[23] and its IR spectrum (523 K)[28] are also included.

In Figure 6 two peaks can be seen for α-AgI: the 3 THz (Raman, IR) peak attributed to optical phonons[23,24,30,31] and a low-frequency peak at 0.9 THz (Raman) and ≈0.7 THz (IR) whose origin is controversial. Four explanations are given in the literature. According to refs 23, 30, 31, and 32, the strong disorder in the distribution of the silver ions breaks the optical and acoustical selection rules for phonons. Hanson et al.[24] attribute the low-frequency peak in α-AgI to the diffusive motions of the silver ions. Winterling et al.[33] suggest two contributions: a narrow component reflecting the diffusive motion of the silver ions and a broader peak linked to local motions of the silver ions at interstitial sites. Finally, Funke et al.,[34] taking into consideration results from other crystals containing silver ions, propose damped large-amplitude oscillations of silver ions within broad potentials.

The IR spectrum of the glass below ≈8 THz shows a very broad vibrational regime. Such broad vibrational features of glasses are often decomposed into Gaussians which are then interpreted in terms of local motions of ionic species on different sites.[20−22] A different approach[39−41] is to decompose the broad vibrational peak into components which are solutions of the Langevin equation.[42] These solutions describe damped harmonic vibrations of single particles in a broad potential. All these different approaches, however, neglect any possible collective character of the vibrations. Attempts to fit the present IR spectra using the latter approach show that the vibrational part has to be decomposed into at least three components, centered at 1.1, 2.2, and 3.6 THz.[41,43] Almost identical peak positions are found in the conductivity spectra of $0.5AgI \cdot 0.5AgPO_3$ glasses.[41] The low-frequency component at ≈1 THz seen in many silver ion conductors might be due to vibrations of silver ions at local sites, whereas the rest of the vibrational spectrum is due either to collective modes or to rattling motions of ions at inequivalent sites.

Figure 7 shows the temperature dependence of the IR spectra of $0.48(AgI)_2 \cdot 0.52Ag_2SeO_4$. The temperature dependence is rather small at frequencies above 1 THz, but strong in the far infrared. The slope in the log−log plot of conductivity versus frequency increases with decreasing temperature and approaches 2 at the lowest temperatures. Slopes of 2 in the very far infrared are typical of pure vibrational components in the conductivity spectra of glasses and crystals, see e.g. refs 2 and 35−38. Slopes smaller than 2 result from a superposition of vibrational and ionic hopping contributions to the dynamic conductivity, the latter becoming more pronounced with increasing temperature.

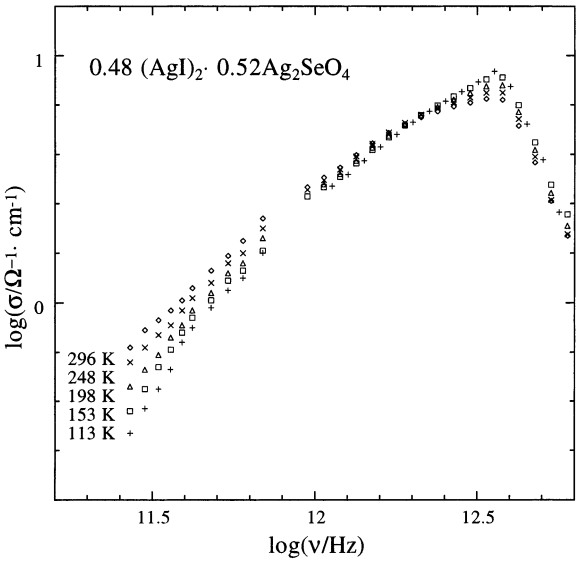

Figure 7. Far-IR range of the dynamic conductivities of glassy $0.48(AgI)_2 \cdot 0.52Ag_2SeO_4$ at various temperatures.

Hopping processes occurring in the glasses studied here are discussed in detail in ref 2.

Conclusions

We have presented the first Raman spectra of crystalline silver selenate and of $x(AgI)_2 \cdot (1 - x)Ag_2SeO_4$ glasses from room temperature up to 573 K covering the glassy, partially crystallized and liquid states.

Peaks at wavenumbers larger than 300 cm^{-1} are due to internal vibrations of the selenate tetrahedra. For orthorhombic c-Ag_2SeO_4, these peaks have been assigned to nine Raman modes. The partially crystallized glasses showed spectra which deviate from those of the glass and the melt reflecting a change in the symmetry of the local environment of the selenate tetrahedra during the partial crystallization.

At wavenumbers lower than 300 cm^{-1} the Raman spectrum of c-Ag_2SeO_4 is determined by lattice vibrations. The normalized Raman spectra of the glasses and of α-AgI are similar. The peak centered at 118 cm^{-1} for $x = 0.35$ increases in intensity and shifts to lower wavenumbers with increasing x. Extrapolation to $x = 1$ yields a wavenumber of 101 cm^{-1} close to the corresponding peak in α-AgI. In crystalling α-AgI, the IR, and Raman peak at 100 cm^{-1} is caused by optical phonons while interpretation of the lower-frequency broad peak is controversial.[23,24,30−34]

In the $0.48(AgI)_2 \cdot 0.52Ag_2SeO_4$ glasses, a very broad IR peak is seen at frequencies lower than 8 THz with a maximum at approximately 3.6 THz which corresponds to a clearly resolved Raman peak at 115 cm^{-1}. Although it is difficult to assign specific vibrational modes, collective vibrations similar to the optical and acoustic phonons in α-AgI or damped vibrations of silver ions in broad potentials are likely to be present.

The Raman and IR spectra of $x(AgI)_2 \cdot (1 - x)Ag_2SeO_4$ can be viewed as a composite of a spectral part at low frequencies related to AgI and a part at high frequency which resembles a broadened spectrum of c-Ag_2SeO_4. Comparable results were obtained for AgI-containing silver borate glasses[26] and for $xAgX \cdot (1 - x)AgPO_3$ glasses, with $x =$ I, Br, Cl.[27] The results were interpreted in terms of α-AgI-like clusters.

Our interpretation of the IR and Raman spectra is consistent with the structural model (Figure 1) containing regions I with high selenate and regions II with high iodide content. Since

isolated selenate tetrahedra exist in the glasses, the frequencies of the internal vibrations are expected to be similar to those of c-Ag_2SeO_4 but with a broader variety of environments faced by the SeO_4 tetrahedra. Therefore, broader peaks are expected in the spectra of the glass, which is the case. The average coordination number of silver by iodide ions were for all glasses close to 2,[3] although they may be local regions with a coordination number of 4. The iodide-rich regions (II) shown in Figure 1 are, however, not to be understood as α-AgI-like clusters.

Acknowledgment. We thank D. L. Price and A. Goldbach for inspiring discussions and K. Funke, J. Kellers, B. Roling, and D. Wilmer for many stimulating suggestions over the past years. The crystalline silver selenate used in the glass preparation was synthesized by M. Buscher. The work at ANL was supported by the U.S. Department of Energy, Division of Materials Science, Office of Basic Energy Sciences, under Contract W-31-109-ENG-38. C.C. gratefully acknowledges a fellowship from the Heinrich Hertz Foundation, Germany, during her visit to ANL.

References and Notes

(1) Angell, C. A. *Solid State Ionics* **1983**, *9*−*10*, 3.
(2) Cramer, C.; Buscher, M. *Solid State Ionics* **1998**, *105*, 109.
(3) Cramer, C.; Price, D. L.; Saboungi, M. L. *J. Phys.: Cond. Matter* **1998**, *10*, 6229.
(4) Kunze, D. In *Fast-Ion Transport in Solids, Solid State Batteries Devices*; Proc. NATO Adv. Study Inst.; Van Gool, W. North Holland: Amsterdam, The Netherlands, 1973; p 401.
(5) Minami, T.; Kazuhiro, I.; Tanaka, M. *J. Non.-Cryst. Solids* **1980**, *42*, 469.
(6) Rao, K. J. *Rev. Solid State Sci.* **1987**, *1*(1), 55.
(7) Shastry, M. C.; Rao, K. J. *Proc. Indian Acad. Sci. Chem. Sci.* **1990**, *102*, 541.
(8) Frebel, D. Diploma Thesis, Münster, 1995.
(9) Hoppe, R.; Kloidt, T.; Funke, K. *Ber. Bunsenges. Phys. Chem.* **1991**, *95*, 1025.
(10) Roling, B.; Funke, K. *J. Non-Cryst. Solids* **1997**, *212*, 1.
(11) Spitzer, W. G.; Miller, R. C.; Kleimann, D. A.; Howart, L. E. *Phys. Rev.* **1962**, *126*, 1710.
(12) Wu, G. J.; Frech, R. *J. Chem. Phys.* **1977**, *66*, 1352.
(13) Choi, B.-K.; Lockwood, D. L. *Solid State Commun.* **1989**, *72*, 133.
(14) Park, Y. S.; Frech, R. *Spectrochimica Acta* **1989**, *45*, 213.
(15) Paetzhold, R.; Amoulong, H. *Z. Anorg. Allg. Chem.* **1965**, *337*, 225.
(16) In order to determine the density of the vibrational states of amorphous solids, the Raman intensities are not only normalized by the factor $n(\tilde{\nu}) + 1$ (as commonly done for crystals), but by an additional factor $C(\tilde{\nu})/\tilde{\nu}$ where $C(\tilde{\nu})$ is the "coupling constant". In the first model developed by Shuker and Gammon it was supposed that $C(\tilde{\nu}) = \text{const.}$[17] Later, Martin and Brenig showed that $C(\tilde{\nu})$ should vary as $\tilde{\nu}^2$.[18] There is an ongoing discussion about the correct expression for $C(\tilde{\nu})$, in ref 19 and references given therein. Since we are not interested in the exact form of the density of states, we focus on the elimination of the explicitly statistical factor $n(\tilde{\nu}) + 1$ only. The resulting spectra are then compared with those of crystalline compounds, like α-AgI.
(17) Shuker, R.; Gammon, R. W. *Phys. Rev. Lett.* **1970**, *4*, 222.
(18) Martin, A. J.; Brenig, W. *Phys. Status Solidi B* **1974**, *64*, 163.
(19) Sokolov, A. P.; Kisliuk, A.; Quitmann, D.; Duval, E. *Phys. Rev. B* **1993**, *48*, 7692.
(20) Kamitsos, E. I.; Patsis, A.; Karakassides, M. A.; Chryssikos, G. D. *J. Non-Cryst. Solids* **1990**, *126*, 52.
(21) Ingram, M. D.; Chryssikos, G. D.; Kamitsos, E. I. *J. Non-Cryst. Solids* **1991**, *1089*, 131−133.
(22) Kamitsos, E. I.; Kapoutsis, J. A.; Chryssikos, G. D.; Hutchinson, J. M.; Pappin, A. J.; Ingram, M. D.; Duffy, J. A. *Phys. Chem. Glasses* **1995**, *36*, 141.
(23) Delaney, M. J.; Ushioda, S. *Solid State Commun.* **1976**, **19**, 297.
(24) Hanson, R. C.; Fjeldly, T. A.; Hochheimer, H. D. *Phys. Status Solidi B* **1975**, *70*, 567.
(25) Fontana, A.; Mariotto, G.; Fontana, M. P. *Phys. Rev. B* **1980**, *21*, 1102.
(26) Fontana, A.; Mariotto, G.; Cazzanelli, E.; Carini, C.; Cutroni, M.; Frederico, M. *Phys. Lett.* **1983**, *93A*, 209.
(27) Malugani, J.-P.; Mercier, R. *Solid State Ionics* **1984**, *13*, 293.
(28) Jost, W.; Funke, K.; Jost, A. *Z. Naturforsch.* **1970**, *25*, 943.
(29) Funke, K.; Jost, A. *Ber. Bunsenges. Phys. Chem. 1971*, *75*, 436.
(30) Brüesch, P.; Bührer, W.; Smeets, H. J. M. *Phys. Rev. B* **1980**, *22*, 970.
(31) Cazzanelli, E.; Fontana, A.; Mariotto, G.; Mazzacurati, V.; Ruocco, G.; Signorelli, G. *Phys. Rev. B.* **1983**, *28*, 7269.
(32) Alben, R.; Burns, G. *Phys. Rev. B* **1977**, *16*, 3746.
(33) Winterling, G.; Senn, W.; Grimsditch, M.; Katiyar, R. *Proceedings of the International Conference on Lattice Dynamics*; Balkanski, M., Ed.; Flammarion: Paris, 1977; p 553.
(34) Funke, K.; Wilmer, D.; Lauxtermann, T.; Holzgreve, R.; Bennington, S. M. *Solid State Ionics* **1996**, *86*−*88*, 141.
(35) Strom, U.; Hendrickson, J. R.; Wagner, R. J.; Taylor, P. C. *Solid State Commun.* **1974**, *15*, 1871.
(36) Strom, U.; Taylor, P. C. *Phys. Rev. B* **1977**, *16*, 5512.
(37) Cramer, C.; Funke, K.; Saatkamp, T. *Philos. Mag. B. 1995*, *71*, 701.
(38) Cramer, C. *Ber. Bunsenges. Phys. Chem. 1996*, *100*, 1497.
(39) Cramer, C.; Funke, K.; Vortkamp-Rückert, C.; Dianoux, A. J. *Physica A* **1992**, *191*, 358.
(40) Saatkamp, T. Ph.D. Thesis, Münster, 1997.
(41) Cramer, C.; El-Egili, K. A. I.; Funke, K.; Gockel, J.; Grüter-Höge, E.; Holtwick, R.; Lange, M.; Püschel, R.; Zurwellen, D. to be published in *Ber. Bunsenges. Phys. Chem.*
(42) Reif, F. *Fundamentals of Statistical and Thermal Physics*; McGraw-Hill Book Co.: Singapore, 1965.
(43) Buscher, M. Ph.D. Thesis, Münster, 1997.
(44) Cava, R. J.; Reidinger, F.; Wuensch, B. J. *Solid State Commun.* **1977**, *24*, 411.
(45) Swenson, J.; McGreevy, R. L.; Börjesson, L.; Wicks, J. D.; Howells, W. S. *J. Phys. 1996*, *8*, 3545.